Educational inequalities in extreme heat-related mortality across Belgian districts

Abstract

Background: Climate change is increasing the frequency and intensity of extreme heat events, with disproportionate impacts on vulnerable populations. Educational attainment shapes heat vulnerability through multiple pathways — including health literacy, thermoregulatory behaviour, and access to protective resources — yet evidence on educational gradients in heat-related mortality remains limited.

Methods: Using Belgian mortality records linked to educational attainment for adults aged 60 and over (2002–2019), we applied a two-stage distributed lag non-linear modelling framework across 42 NUTS-3 districts and three educational groups. First-stage models estimated district- and education-specific exposure-response functions; second-stage multivariate meta-regression pooled these estimates and quantified the educational gradient in heat vulnerability. Attributable mortality was computed for extreme heat days, defined as days exceeding the 97.5th national temperature percentile (28.3°C), and expressed as age-standardised rates per 100,000 person-years.

Results: A clear educational gradient in extreme heat vulnerability emerges, with relative risks at the 99th percentile of 1.28 (95% CI: 1.12–1.31), 1.22 (95% CI: 1.12–1.25), and 1.16 (95% CI: 1.09–1.22) for the low, secondary, and tertiary education groups respectively. Age-standardised heat-attributable mortality rates during extreme heat days are 26.5, 19.4, and 13.0 per 100,000 person-years, with non-overlapping confidence intervals between the lowest and the two higher education groups. The gradient is consistent across all 42 districts, though district-level differences are not always statistically distinguishable given sample sizes. Model selection indicates that individual educational attainment alone characterises between-district heterogeneity in heat vulnerability, with no additional explanatory gain from area-level deprivation indices.

Conclusions: Educational attainment is a significant modifier of extreme heat vulnerability among older adults in Belgium, operating primarily through individual-level pathways rather than geographic context alone. As extreme heat becomes more frequent under climate change, the unequal burden documented here is likely to intensify, underscoring the need for targeted heat policies that account for individual-level vulnerability.

Keywords: Climate change, Mortality, Inequalities, Socio-economic status

1 Background

Climate change is intensifying the frequency and severity of extreme heat events, with growing consequences for human health (Calvin et al. 2023). Evidence suggests that the burden of heat-related mortality may not be shared equally across populations, with socioeconomic position potentially shaping exposure, vulnerability, and adaptive capacity. However, the socioeconomic determinants of temperature-related mortality remain poorly documented, and the existing evidence base is limited (Benmarhnia et al. 2015). Educational attainment may be one such modifier, though the mechanisms and magnitude of its influence on heat vulnerability remain poorly established. This study examines how educational attainment modifies the relationship between temperature and mortality among the elderly across Belgian districts, and whether this reflects a broader socio-spatial gradient in vulnerability.

1.1 Temperature and mortality

Non-optimal temperatures are responsible for a substantial share of global mortality. Zhao et al. (2021) estimated that over 5 million deaths annually — 9.43% of global mortality — are attributable to temperatures outside an optimal range, with cold-related deaths (8.52%) far outnumbering heat-related ones (0.91%). Critically, however, heat-related mortality is rising, in line with observed warming trends (Zhao et al. 2021). Temperature affects mortality through several physiological pathways, most notably cardiovascular and respiratory ones: both extreme heat and cold elevate risks of cardiovascular death, ischaemic heart disease, stroke, and heart failure (Alahmad et al. 2023), while in Belgium the strongest associations have been observed for respiratory causes (Demoury et al. 2022).

Central to this literature is the concept of the minimum mortality temperature (MMT) — the temperature at which mortality risk is lowest. The temperature-mortality relationship is typically U- or V-shaped around the MMT, with risk increasing at both cold and hot extremes (Gosling et al. 2009). The MMT varies geographically but generally aligns with local average temperatures, reflecting population acclimatisation to local climate conditions (Yin et al. 2019). Temperature effects are also distributed across time, with mortality impacts occurring days after exposure, requiring analytical approaches that account for these delayed effects (Gosling et al. 2009), there heat effects tend to occur within days of the recorded temperatures, whereas cold related deaths often occur at longer lags (Anderson and Bell 2009). In this study, daily maximum temperature serves as the exposure measure, given its direct relevance to heat stress and consistent availability across Belgian meteorological records (Barnett et al. 2010). Finally, ongoing population ageing substantially modifies the temperature-mortality burden, amplifying heat-related effects — a dynamic particularly relevant in ageing European populations (de Schrijver et al. 2022).

1.2 Education, socioeconomic status, and heat vulnerability

Heat-related mortality is shaped by both individual characteristics and behaviours. In their review, Gagnon et al. (2026) identify thermoregulatory behaviour — such as reducing physical activity, seeking shade, or using cooling — as the primary driver of

differential vulnerability, alongside personal characteristics. Differential exposure also plays a role: outdoor workers, residents of urban heat islands, and those in precarious or poorly insulated housing face higher heat loads and are therefore at greater risk.

Individual socioeconomic characteristics modify the temperature-mortality relationship, and the evidence consistently points toward greater vulnerability among lower socioeconomic groups, though patterns are complex and context-dependent (Son et al. 2019). In a large meta-analysis, Balaj et al. (2024) document that adults with 12 years of schooling face a 24.5% lower all-cause mortality risk than those with no schooling, with each additional year of education associated with a 1.9% reduction. Whether comparable gradients extend to heat-specific mortality remains an open question. The available studies offer a mixed but suggestive picture: Marí-Dell'Olmo et al. (2019) document an educational gradient in temperature-related mortality in Barcelona, though with notable sex differences and a non-monotonic pattern among men; in Turin, Ellena et al. (2020) find the highest heat-related mortality risk among low-educated women, with no equivalent gradient among men. Conte Keivabu (2022) show that in Spain, individuals in lower socioeconomic positions face increased mortality risks at both temperature extremes, whereas no significant association is observed among the more advantaged. Beyond education, Conte Keivabu et al. (2024) find that ethnic minorities in the United States face disproportionately higher mortality on hot days, pointing to the broader role of socially structured vulnerability.

Several pathways could explain such a gradient. Lutz and Muttarak (2017) synthesise evidence that education enhances cognitive development, risk assessment, and future planning — capacities directly relevant to climate adaptation. Education also fosters health literacy (Fan et al. 2021) and social capital (Huang et al. 2009), while the higher incomes associated with higher educational attainment enable investment in protective resources such as cooling infrastructure. More broadly, as Eggerickx et al. (2020) note, educational level captures knowledge and cultural capital that shape healthcare access and prevention behaviours. This makes educational attainment an effective marker of the socioeconomic mechanisms through which vulnerability to heat may be differentially distributed.

1.3 Study area

Belgium is divided into three administrative regions — Flanders, Wallonia, and the Brussels-Capital Region — themselves subdivided into 44 districts, as shown in Figure 1. Belgium presents a particularly suitable case study for this analysis, given its well-documented geographic and socioeconomic health inequalities. Life expectancy has been rising, but mortality inequalities have intensified: while the gender gap has narrowed, socioeconomic disparities have widened, and spatial disparities in mortality at the district level have been worsening for at least the past quarter century (Eggerickx et al. 2020). Area-level deprivation also follows a clear geographic pattern, with hotspots concentrated in Wallonia, as documented by the Belgian Indices of Multiple Deprivation (Otavova et al. 2023). These spatial inequalities translate directly into mortality differentials: residents of more deprived areas face higher risks of premature death (Otavova et al. 2024). Furthermore, all-cause mortality rates among men are systematically higher in Wallonia and the Brussels-Capital Region than in Flanders,

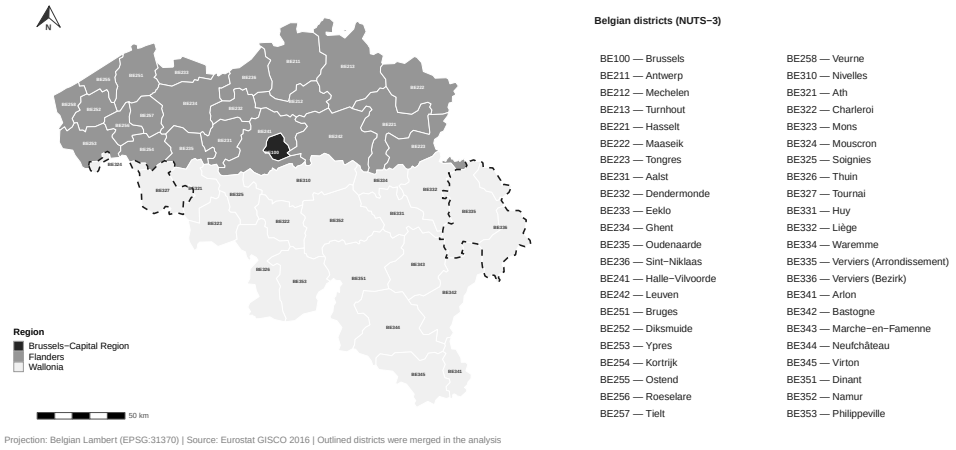

Fig. 1: The 44 Belgian districts (NUTS3 level) across the three administrative regions.

with the highest rates in Brussels inner city areas and several Walloon cities — partly attributable to the lower socioeconomic positioning of residents (Van Hemelrijck et al. 2016). Among men, higher educational attainment is associated with mortality rates two to three times lower than among the least educated (De Grande et al. 2014). Heat-related mortality in Brussels is moreover projected to rise due to both climatic and demographic changes (Crouzier et al. 2024), and while this likely reflects broader national trends, the differential impact across socioeconomic groups across Belgium remains insufficiently studied (Demoury et al. 2022).

2 Data

2.1 Temperature data

Daily maximum temperature data were obtained from the Royal Meteorological Institute of Belgium for the period 1992–2022. The original data were provided as gridded pixels defined by longitude and latitude coordinates, which were converted into spatial features and projected into a consistent coordinate reference system (EPSG:4326) to ensure compatibility with the NUTS-3[1] district boundaries. Each temperature grid point was then assigned to its corresponding NUTS-3 unit via spatial join, with a nearest-neighbour fallback applied to pixels not covered by any district polygon, enabling aggregation of daily maximum temperatures at the district level. The distribution of mean daily maximum temperatures across districts over the study period is shown in Figure A1 in the Appendix. The temperature distribution of the analytical districts are very similar with mean daily maximum temperatures ranging from 12.84°C in Bastogne to 15.63°C in Maaseik over the observation period. Temperature exposure was characterised using daily maximum temperature (°C) with a maximum lag of seven days, to capture the more immediate effects of heat on mortality.

[1] Results are presented using the 2016 NUTS boundaries.

2.2 Mortality data

Educational attainment was categorised into three levels: low (no formal education, primary, and lower secondary schooling), secondary (upper secondary and post-secondary non-tertiary), and tertiary (Bachelor's, Master's, and Doctoral level). Educational attainment was derived from the 2001 Belgian census and individual-level death records obtained from the Belgian Statistical Office (StatBEL). The analysis was restricted to individuals aged 60 and over, both to ensure sufficient numbers of deaths for stable estimates and because educational attainment recorded at death may be incomplete for individuals who died before completing their educational trajectory.

The distribution of deaths across educational groups is shown in Tables A1, A2 and A3 in the Appendix. Over the study period 2002–2019, a total of 1,392,134 deaths were recorded among individuals with known educational attainment. The low education group accounted for the large majority of these (n = 1,047,639; 62.6%), reflecting both their greater numbers in the older Belgian population and their higher observed mortality: 3,853.9 deaths per 100,000 person-years, compared to 2,480.8 and 1,927.7 in the secondary and tertiary groups respectively. An additional 280,957 deaths (16.8%) could not be linked to an educational record and were excluded from the analysis. The robustness of results to this exclusion was assessed by reassigning unknown deaths to educational groups under two alternative assumptions; results are presented in Section D.1 of the Appendix and confirm that the educational gradient is not sensitive to the treatment of missing attainment. The age distribution of deaths also differed across groups: 41.2% of deaths in the low education group occurred at age 85 or above, compared to 33.3% and 32.8% in the secondary and tertiary groups.

To maintain a consistent exposure classification throughout follow-up, the study population was restricted to individuals enumerated in the 2001 census, forming a closed cohort. Each death record was linked to its corresponding census-based educational classification, and individuals were followed from January 2002 or the calendar year in which they turned 60, until death or end of follow-up in 2019. Where educational attainment was missing from the census, the value recorded on the death certificate was used as a substitute. Individuals with no educational information in either source were excluded from the analysis.

Person-years at risk were computed for each individual as the time lived within the study window, aggregated by district, educational group, and five-year age band, and used as the denominator for age-specific mortality rates. Standard population weights were derived from the national within-education age distribution of the 2011 Belgian census and used subsequently for the direct age standardisation of heat-attributable mortality rates by educational attainment.

2.3 Meta-predictors - Belgian Indices of Multiple Deprivation

District-level meta-predictor variables were compiled to characterise the socioeconomic context of each analytical unit. Domain-specific deprivation scores from the Belgian Index of Multiple Deprivation (Otavova et al. 2023) were used, capturing area-level variation in income, employment, education, housing, crime, and health. Scores were originally computed at the statistical sector level and aggregated to NUTS-3 districts

using population-weighted means prior to inclusion in the second-stage meta-regression as potential modifiers of the education-temperature-mortality relationship.

3 Methods

We applied the two-stage analytical framework developed by Masselot and Gasparrini (2025) for multi-location studies of temperature-related mortality. In the first stage, non-linear and lagged temperature-mortality associations are estimated separately for each district-education combination using distributed lag non-linear models (DLNMs). In the second stage, district-level estimates are pooled through a multivariate meta-regression that produces population-average exposure-response functions by educational group and location-specific refinements via Best Linear Unbiased Predictions (BLUPs). The framework explicitly propagates first-stage estimation uncertainty into the second stage. The primary adaptation relative to the original implementation is the use of educational attainment as the stratification dimension, replacing the age-group stratification used by Masselot and Gasparrini (2025). Since the analysis covers the full Belgian population with no unobserved locations, the spatial prediction component of the framework was not required. Full methodological details are provided in Appendix B.

3.1 Study design and stratification

Educational attainment serves as the primary stratification dimension throughout. First-stage models were fitted for each combination of district and educational attainment level, yielding 126 district- and education-specific exposure response functions across 42[2] analytical districts and 3 education groups. Age and sex are well-documented modifiers of temperature vulnerability, but their inclusion as additional stratification dimensions was not feasible given the already high degree of stratification introduced by district and educational attainment: further subdivision reduced death counts within each cell to levels incompatible with stable first-stage estimates. The restriction to adults aged 60 and over partially addresses age heterogeneity by focusing on the population at greatest risk. While exposure-response functions are estimated across the full temperature range, results are reported exclusively for heat-attributable mortality, defined as mortality occurring on days above the common MMT.

3.2 Temperature exposure and lag structure

The DLNM was fitted over the full temperature range to enable identification of the MMT, which serves as the reference point for all heat-related estimates. A maximum lag of seven days was applied, reflecting the short biological timescale of heat-related mortality, for which physiological effects are concentrated within the first few days following exposure, while cold-related mortality is known to exhibit longer

[2]Two administrative mergers were applied to ensure model convergence. Mouscron (BE324) was merged into Tournai (BE327), reflecting their administrative consolidation in 2018. The two Verviers sub-units (BE335 and BE336) were merged into a single analytical unit due to insufficient death counts. For mapped results, all 44 districts are displayed, with merged units assigned identical estimates. Temperatures were averaged and death counts summed across merged units.

lag structures (Anderson and Bell 2009). The present analysis focuses exclusively on heat-attributable mortality. This focus is motivated by evidence that cold-related mortality is strongly seasonal and unlikely to diminish substantially under climate change, given its dependence on respiratory and cardiovascular disease pathways that are not solely linked to temperature (Willem et al. 2012), whereas heat-related mortality is projected to increase substantially under warming scenarios (Lüthi et al. 2023). Sensitivity analyses using lags of 14 and 21 days confirm that the educational gradient in heat vulnerability is robust to this choice (Appendix D.2).

3.3 Minimum mortality temperature

Education-specific pooled exposure-response functions were expressed on a common national temperature scale. The MMT was identified as the temperature at which each education-specific curve reached its minimum, within a pre-specified search window (25th–99th national percentile[3]). Education-specific MMTs ranged from 15.8°C (53rd percentile) in the tertiary group to 21.4°C (79th percentile) in the low education group. Between the 25th and 75th national temperature percentiles, relative risks are close to null and confidence intervals include one across all education groups, indicating no meaningful excess mortality in this range and rendering the precise location of the MMT within it of negligible consequence. Using education-specific MMTs as centering points would nonetheless render the exposure-response functions non-comparable across groups, as each curve would express risk relative to a different reference temperature. A common MMT of 21.0°C (77th national percentile) was therefore defined as the median across groups and used as the shared centering point for all exposure-response functions, such that relative risk (RR) = 1 at this reference temperature by construction, enabling direct comparison across educational groups.

3.4 Extreme heat-attributable mortality

While attributable deaths are estimated across the full heat range, results are reported exclusively for extreme heat days. Definitions of extreme temperature vary widely in the literature, spanning heatwave events with duration criteria, fixed absolute thresholds, and various percentile cut-offs (Xu et al. 2016). We define extreme heat at the day level rather than the event level, using the 97.5th national percentile of daily maximum temperature (28.3°C) as the threshold. The 99th percentile, used in some studies (Alahmad et al. 2023), captures only the uppermost 1% of the observed distribution and is subject to considerable uncertainty given the scarcity of observations at those extremes. The 97.5th percentile offers a more stable estimate while remaining well within the extreme range, and aligns with the threshold used by Demoury et al. (2022) in a comparable Belgian study, facilitating direct comparison.

For each district i and educational group e, daily attributable deaths were computed from the BLUP-corrected exposure-response function and summed over days exceeding the 97.5th national percentile to obtain total extreme heat-attributable

[3]The sensitivity of results to the MMP range was assessed across four alternative specifications: (10th–99th), (50th–99th), (25th–95th), and (25th–90th) percentiles. The common MMT was stable across all specifications.

numbers. The overall attributable fraction was derived as the ratio of attributable to total deaths over the study period.

3.5 Age standardisation

Age-standardised heat-attributable mortality rates (ASMR), expressed per 100,000 person-years, were computed using direct standardisation to enable comparison across districts and educational groups with different age compositions. For each district-education stratum, age specific all-cause mortality rates were weighted by the national Belgian 2011 census age distribution, used as a common standard population across all educational groups. Heat-attributable rates were then obtained by applying the attributable fraction to the age-standardised all-cause rate. This approach assumes that the attributable fraction is constant across age groups within each district-education cell.

3.6 Uncertainty quantification

Uncertainty in all extreme heat-attributable mortality estimates was quantified through Monte Carlo simulation with 1,000 iterations. At each iteration, coefficients were drawn jointly from the multivariate normal distribution defined by the meta-regression fixed effects and their variance-covariance matrix, and independently from the district-level random effect distribution $\mathcal{N}(\mathbf{0}, \hat{\Psi})$. For each simulation draw, attributable fractions and standardised mortality rates were recomputed, and empirical 95% confidence intervals were derived from the resulting simulation distributions.

4 Results

4.1 Educational gradients in extreme heat mortality

The two-stage meta-regression framework yields national-level exposure-response functions by educational attainment through a set of B-spline basis functions, each contributing differently across the temperature distribution. The shapes of these basis functions, their relative contributions at each temperature percentile, and the coefficients capturing the step change between educational attainment levels are shown in panels A, C, and B of Figure 2, respectively.

Educational attainment is modelled as a linear step (low = 1, secondary = 2, tertiary = 3), such that each spline coefficient represents the change in log-relative risk per unit increase in educational attainment. Negative coefficients indicate that higher education is associated with lower mortality risk. Overall, all coefficients are negative, suggesting a broadly protective gradient across the temperature range, though coefficients b1 through b4 all include zero within their 95% confidence intervals. The exception is b5, which defines the shape of the exposure-response function at the extreme heat end of the distribution and is the only statistically significant coefficient ($\hat{\beta}_5 = -0.37$; 95% CI: -0.16, -0.57). Since b5 defines the exposure response function for the temperature range above the 97.5th percentile (panel C), the educational gradient in mortality risk emerges precisely at the temperatures of greatest concern.

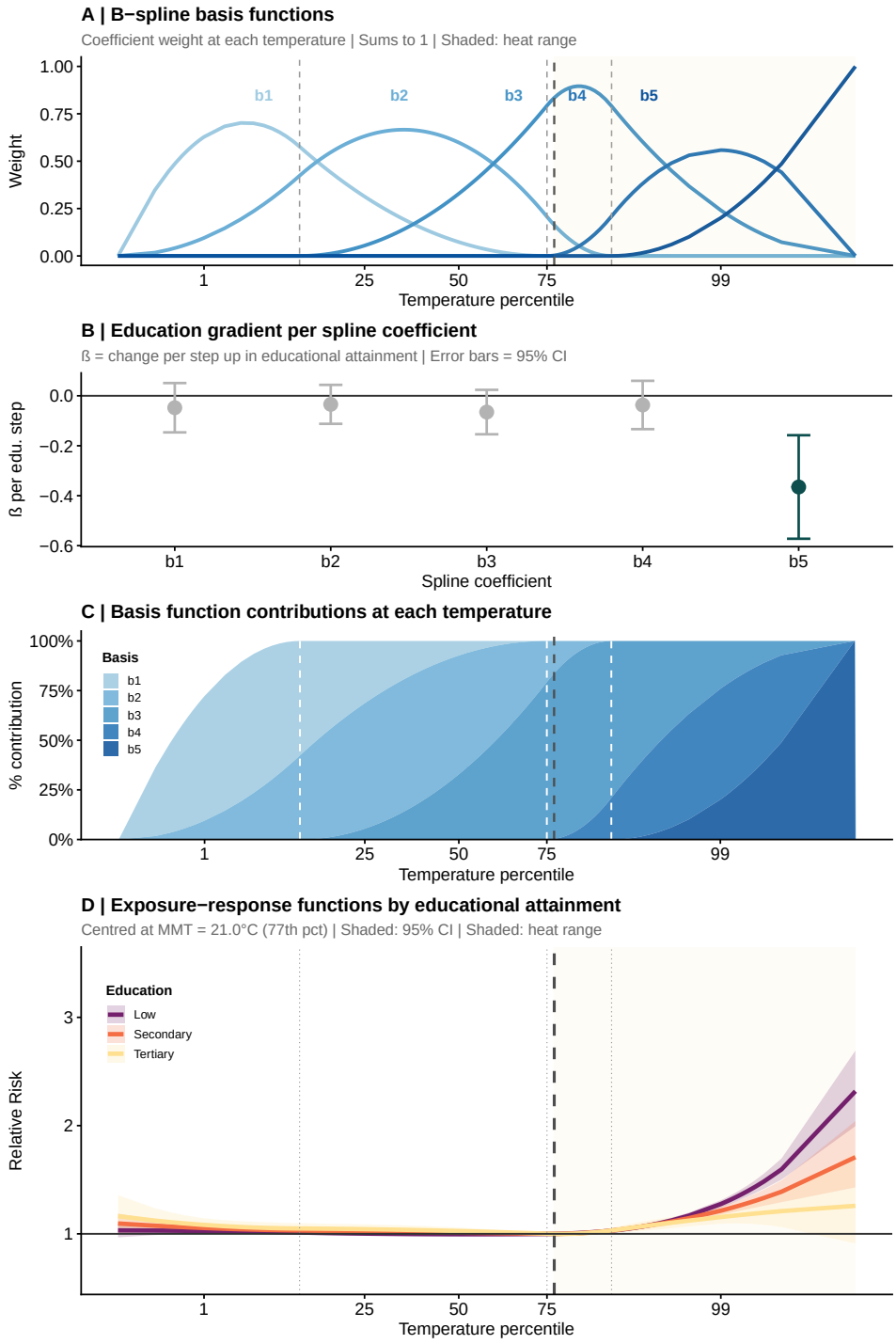

Fig. 2: Temperature-mortality exposure-response functions by educational attainment and their spline decomposition. Belgians aged 60 and over, 2002-2019.

This pattern is visible in the exposure-response curves in panel D of Figure 2. Across most of the temperature distribution, the three educational groups show broadly similar relative risks with overlapping confidence intervals, and it is worth noting that the gradient is not monotonically ordered below the MMT. Differences widen markedly above the 98th percentile, with the low education group facing the highest risk. At the 99th percentile, the relative risk of mortality is 1.28 (95% CI: 1.242–1.311) for the lowest education group, 1.22 (95% CI: 1.176–1.253) for the secondary group, and 1.16 (95% CI: 1.094–1.221) for the tertiary group. Numerical estimates across the full temperature range, are provided in Table C4 in the Appendix.

4.2 Intensifying socio-spatial extreme-heat mortality disparities under climate change

Focusing on extreme heat days — defined here as days exceeding the 97.5th national temperature percentile (28.3°C) — a clear educational gradient in heat-attributable mortality emerges. Panel A of Figure 3 shows the national exposure-response functions in the heat range: above 33°C, mortality risk increases markedly for the low and secondary education groups, while the tertiary group shows a flatter response with widening uncertainty. Translating these relative risks into mortality rates, age-standardised heat-attributable mortality rates during extreme heat days are 26.46 (95% CI: 22.40–27.63), 19.37 (95% CI: 15.54–21.76), and 12.96 (95% CI: 7.97–16.17) per 100,000 person-years for the low, secondary, and tertiary education groups respectively (Table C5). The low education group faces more than twice the mortality rate of the tertiary group. At the national level, the confidence intervals of the secondary and tertiary groups do not overlap with that of the low education group, providing statistical evidence of a meaningful gradient in extreme heat vulnerability across educational levels. The difference between the secondary and tertiary groups is more modest and their confidence intervals partially overlap, suggesting a clearer distinction between those with no or limited formal education and those with at least a secondary qualification than between the two higher groups.

Comparing standardised to crude rates reveals the importance of age adjustment (see Table C5). Standardisation increases estimates for the secondary and tertiary groups by 6.80 and 5.39 per 100,000 person-years respectively, reflecting their relatively younger age composition within the 60-and-over population. The two measures capture different but complementary aspects of inequality. Crude rates reflect the mortality differentials actually occurring across the Belgian 60-and-over population during the study period: because lower-educated individuals are older on average, their crude rates are higher and the ratio between the least and most educated groups comes up to a factor of three. Age-standardised rates, by contrast, hold age structure constant and isolate differential heat vulnerability independent of demographic composition, this yields more conservative estimates that single out the differences in risk in the educational gradient.

This gradient is all the more concerning in the context of ongoing warming. Panel B of Figure 3 shows the distribution of monthly maximum temperatures (TXx) between May and September across two reference periods (1992–2002 and 2012–2022). The distribution has shifted rightward over time, with recent years producing TXx values

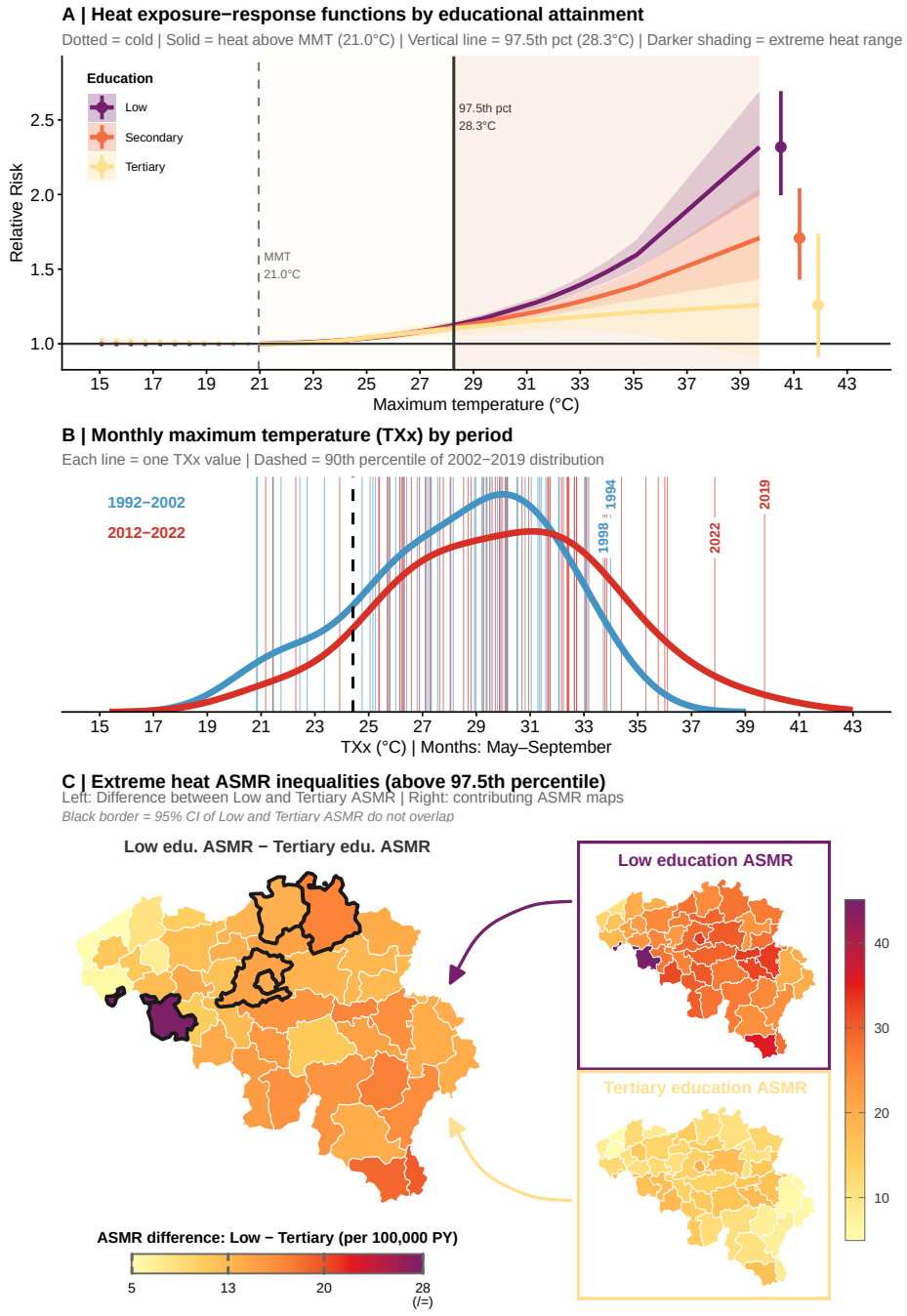

Fig. 3: Heat vulnerability by educational attainment: exposure-response functions, shifting temperature distributions, and geographic distribution of extreme heat mortality inequalities across Belgian districts. Belgians aged 60 and over, 2002–2019.

that increasingly exceed the extreme heat threshold. Notable events such as the 2019 and 2022 heatwaves are visible as individual observations in the upper tail. Under continued climate change, days qualifying as extreme under the current threshold are projected to become more frequent, directly amplifying the mortality burden that disproportionately affects lower-educated groups.

At the district level, between-district heterogeneity in the temperature-mortality relationship is low ($I^2 = 8.4\%$, 95% CI: 0.0%–19.5%), suggesting that the educational gradient in heat vulnerability is broadly consistent across Belgium rather than driven by a small number of outlying districts. Nonetheless, the geographic distribution of absolute mortality inequalities reveals meaningful spatial patterns. The difference in age-standardised heat-attributable mortality rates between the low and tertiary education groups (panel C of Figure 3) is largest in the west — particularly in the Tournai-Mouscron district — and in the south, notably in Virton and Arlon. The Brussels-Capital Region presents a contrasting profile: high absolute mortality rates in the low education group but a more modest contrast between educational groups, illustrating that the magnitude of the inequality does not always track the absolute level of risk. Districts outlined in the comparison map are those where the 95% confidence intervals of the low and tertiary education age standardised mortality rate estimates do not overlap, indicating statistically distinguishable differences. These districts tend to be some of the more densely populated, where larger death counts yield sufficient statistical power to detect the gradient. Across all districts without exception, the point estimate of the difference is positive, indicating that the low education group consistently shows higher extreme heat mortality than the tertiary group.

5 Discussion

5.1 Main findings

Heat-related mortality risk in Belgium follows a clear educational gradient, with the lowest-educated group consistently more vulnerable at extreme temperatures. The relative risks we estimate — 1.28, 1.21, and 1.15 at the 99th percentile for the low, secondary, and tertiary groups — are coherent with the existing Belgian literature. Demoury et al. (2022) report a relative risk of 1.21 (95% CI: 1.08–1.36) at a comparable percentile for Belgian agglomerations using a 21-day lag, while Demoury et al. (2022), working on a national dataset with a seven-day lag, find an odds ratio of 1.17 (95% CI: 1.12–1.21) at the 97.5th percentile with an MMT of 21.1°C — closely matching our 21.0°C. At the European scale, Janoš et al. (2025) place Belgian regional estimates between 1.1 and 1.3 at the 99th percentile for adults aged 75 and over, a range within which our results sit.

The educational gradient we document extends findings from Spain and Italy (Conte Keivabu 2022; Marí-Dell'Olmo et al. 2019; Ellena et al. 2020) to a Belgian context, and shows that differences in heat susceptibility by educational attainment translate into substantial mortality differentials. Age-standardised rates for the low education group are more than twice those of the tertiary group, with non-overlapping confidence intervals at the national level. The persistence of this gradient after standardisation is meaningful: it indicates that the differential is not simply a demographic

artefact of the older age structure of the lower-educated group, but reflects genuine differences in vulnerability. These likely operate through the pathways identified in the literature — differential health literacy shaping thermoregulatory behaviour, unequal access to cooling, and poorer housing conditions (Gagnon et al. 2026) — though this study does not allow us to quantify the relative contribution of each. Crude rates, which approach a factor of three between the lowest and highest groups, tell a complementary story: in the population as it actually exists, older age and lower education compound one another, and this cumulative disadvantage is what determines mortality during extreme heat events in Belgium today.

The spatial dimension adds nuance without altering the main finding. Between-district heterogeneity is low, meaning the gradient is not confined to a handful of atypical locations but is broadly observed across Belgium. Where absolute inequalities are largest — particularly in parts of Wallonia — area-level deprivation and individual vulnerability tend to reinforce one another, consistent with evidence on the geographic concentration of disadvantage in Belgium (Otavova et al. 2023, 2024). The Brussels-Capital Region presents a different configuration: despite meaningful differences between educational groups, the gap is narrower than in some less urbanised districts, while the tertiary-educated group records some of the highest absolute mortality estimates of any district — a pattern consistent with urban heat island effects that expose all residents to elevated temperatures regardless of individual characteristics. Model selection reinforces this interpretation: individual educational attainment alone was sufficient to characterise between-district heterogeneity in heat vulnerability, with no additional explanatory gain from area-level deprivation indices. Place shapes exposure, but individual characteristics remain the primary driver of differential vulnerability.

In a context of rising temperatures, these findings carry implications for future health action. The rightward shift in the distribution of maximum temperatures is projected to continue. More frequent extreme heat days will directly amplify the mortality burden on those already most exposed — older, lower-educated individuals living in the least protective environments. Without targeted intervention, climate change is likely to widen inequalities that are already measured today.

5.2 Limitations

The most substantive limitation concerns the difficulty of fully separating the effect of educational attainment from that of frailty. Lower-educated individuals tend to be older within the 60-and-over group and to have higher baseline mortality (Renard et al. 2017), and these factors cannot be perfectly disentangled with the data available here. Age standardisation addresses compositional differences in age structure across educational groups, but cannot account for differences in health status within age strata. The concentration of the gradient in the extreme heat tail, rather than across the full temperature distribution, is reassuring — a frailty artefact would be expected to shift the entire exposure-response curve upward rather than accelerate it selectively at extreme temperatures — but this reasoning remains suggestive rather than conclusive. Future work incorporating cause-of-death data and finer age stratification would allow a cleaner decomposition of heat vulnerability from underlying health status.

The seven-day lag is appropriate for heat but means the cold range of the exposure-response function is not reliably estimated. Cold-side results should not be interpreted, and the analysis is explicitly scoped to heat-attributable mortality.

A further limitation concerns missing data. Some 16.8% of deaths could not be linked to an educational record and were excluded from the main analysis. Sensitivity analyses reassigning these deaths under alternative assumptions confirm that the educational gradient is robust to their exclusion. Individuals who arrived in Belgium after the 2001 census are similarly absent from the educational linkage. Finally, sex differences in heat vulnerability, which are documented in the literature and likely interact with educational gradients, could not be examined here without reducing cell sizes to levels incompatible with stable first-stage estimation.

Area-level deprivation indices from the Belgian Index of Multiple Deprivation (Otavova et al. 2023) were considered as district-level meta-predictors but did not improve model fit and were excluded from the final specification. Other district-level factors — including green space availability, urban heat exposure, or healthcare infrastructure — were not examined, and may capture dimensions of vulnerability not reflected in the BIMD. That said, the BIMD domains are broad and have recently been shown to correlate with green space inequalities in Flanders (Lee et al. 2026), suggesting that they capture a meaningful share of the local environmental characteristics that might otherwise be considered separately. The absence of additional area-level predictors is therefore unlikely to represent a major gap, though it remains a limitation worth acknowledging.

Finally, Belgium's population is becoming progressively more educated. As the lower-educated group shrinks and its demographic profile changes, the gradient documented here may itself evolve.

5.3 Conclusions

Educational attainment is a meaningful modifier of extreme heat vulnerability among older adults in Belgium. The gradient operates primarily at the individual level, though geography adds a secondary layer of risk in some of the most deprived areas. As extreme heat becomes more frequent, the unequal distribution of vulnerability documented here is likely to intensify. Effective heat policy will need to reach those with the fewest resources to protect themselves — not only through place-based cooling infrastructure, but through interventions that account for the individual characteristics that shape who is most at risk.

6 Acknowledgments

...

Declarations

Funding. Research was supported by funds from the Research Foundation XXX.

Conflict. The authors declare no conflict of interest.

Ethics approval and consent to participate. Not applicable.

Consent for publication. Not applicable.

Data availability. Data are available on reasonable request.

Code availability. Adaptation of the Masselot and Gasparrini (2025) framework with adapted code available on the author's `github`.

Appendix A Descriptive statistics

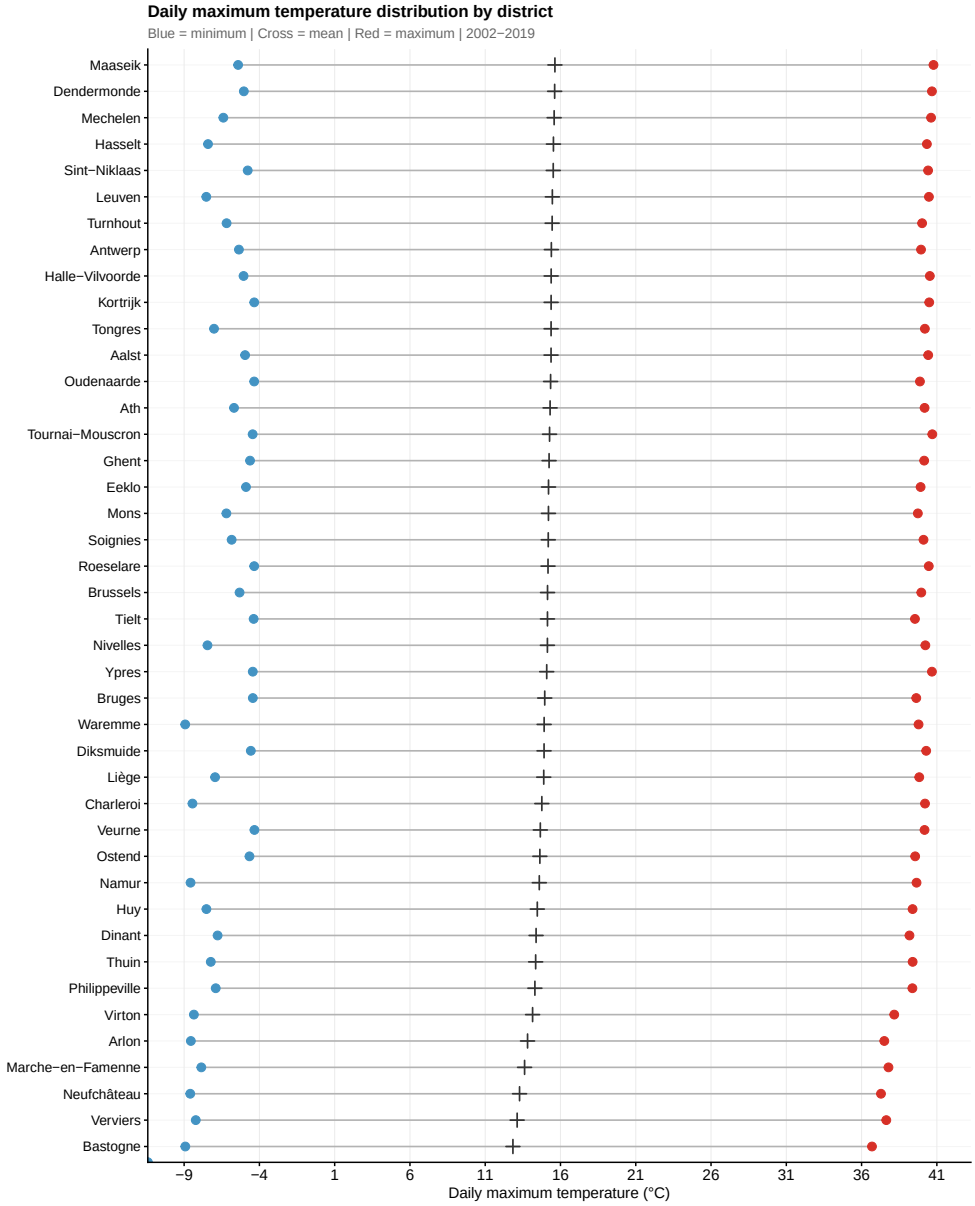

Fig. A1: Distribution of Minimum, Maximum and Mean daily maximum temperature in Belgian districts.

Table A1: Distribution of deaths by educational attainment, Belgian closed cohort 2002–2019, adults aged 60 and over.

Educational attainment	Deaths (n)	Person-years	Deaths (%)	Rate per 100,000 PY
Low	1,047,639	27,183,671	62.6	3853.9
Secondary	201,463	8,121,051	12.0	2480.8
Tertiary	143,032	7,419,985	8.5	1927.7
Unknown/excluded	280,957	/	16.8	/

Table A2: Distribution of deaths by educational attainment and age group, Belgian closed cohort 2002–2019.

	Low		Secondary		Tertiary		Total	
Age group	n	%	n	%	n	%	n	%
60-64	52,678	5.0	20,092	10.0	14,188	9.9	86,958	6.2
65-69	73,326	7.0	21,599	10.7	16,464	11.5	111,389	8.0
70-74	107,386	10.3	24,500	12.2	18,448	12.9	150,334	10.8
75-79	160,785	15.3	30,253	15.0	21,384	15.0	212,422	15.3
80-84	221,700	21.2	37,880	18.8	25,625	17.9	285,205	20.5
85-89	224,115	21.4	36,371	18.1	24,562	17.2	285,048	20.5
90-94	148,919	14.2	22,442	11.1	16,195	11.3	187,556	13.5
95+	58,730	5.6	8,326	4.1	6,166	4.3	73,222	5.3

Table A3: Distribution of deaths by educational attainment and district, including individuals with unknown educational attainment. Belgian closed cohort 2002–2019, adults aged 60 and over.

		Deaths by educational attainment				
Code	District	Low	Secondary	Tertiary	Unknown	Total
BE100	Brussels	71649	22639	20918	31861	147067
BE211	Antwerp	90973	26489	14002	25406	156870
BE212	Mechelen	34134	6543	3621	7129	51427
BE213	Turnhout	39845	6409	3594	8375	58223
BE221	Hasselt	36668	5699	3786	8440	54593
BE222	Maaseik	18336	2552	1636	4462	26986
BE223	Tongres	18821	2560	1558	4344	27283
BE231	Aalst	30883	5158	2612	6042	44695
BE232	Dendermonde	22350	2864	1721	4004	30939
BE233	Eeklo	9926	1122	701	1810	13559
BE234	Ghent	51871	9544	7007	11334	79756
BE235	Oudenaarde	13825	2116	1251	2842	20034
BE236	Sint-Niklaas	24611	2978	2006	5290	34885
BE241	Halle-Vilvoorde	53809	10944	7903	12596	85252
BE242	Leuven	46139	8711	6576	10746	72172
BE251	Bruges	29046	6321	4268	6346	45981
BE252	Diksmuide	6350	465	321	1300	8436
BE253	Ypres	12591	1190	762	2439	16982
BE254	Kortrijk	31382	4320	2730	6344	44776
BE255	Ostend	18209	4064	2285	4169	28727
BE256	Roeselare	16225	1830	1171	2865	22091
BE257	Tielt	10535	974	716	2111	14336
BE258	Veurne	7678	1624	1234	1611	12147
BE310	Nivelles	27982	8156	8165	8780	53083
BE321	Ath	13257	2094	1432	3713	20496
BE322	Charleroi	42954	7008	4866	13576	68404
BE323	Mons	27289	4603	3406	8775	44073
BE324	Mouscron	7369	752	420	2978	11519
BE325	Soignies	17850	2953	2114	5721	28638
BE326	Thuin	17107	2656	1883	5617	27263
BE327	Tournai	17333	2611	2095	5844	27883
BE331	Huy	11141	2192	1550	2971	17854
BE332	Liège	63935	13120	10321	19113	106489
BE334	Waremme	7950	1422	996	1797	12165
BE335	Verviers	26492	4103	3228	9320	43143
BE341	Arlon	4613	754	608	1400	7375
BE342	Bastogne	4120	502	432	1164	6218
BE343	Marche-en-Famenne	5426	843	745	1483	8497
BE344	Neufchâteau	6106	866	708	1925	9605
BE345	Virton	5145	725	588	1446	7904
BE351	Dinant	10889	1973	1614	3195	17671
BE352	Namur	27826	5870	4717	8076	46489
BE353	Philippeville	6999	1144	765	2197	11105

Appendix B Model definition and selection

B.1 First-stage modelling

For each district i and educational level $e \in \{\text{low, secondary, tertiary}\}$, daily mortality counts were modelled as:

$$\log[\mathbb{E}(Y_{iet})] = \alpha_{ie} + f(T_{it},\, \ell;\, \boldsymbol{\theta}_{ie}) + s(t;\, \boldsymbol{\varphi}_{ie}) + \sum_{q=1}^{6} h_q(z_{ieqt};\, \boldsymbol{\gamma}_{ieq}) \tag{B1}$$

where Y_{iet} is the daily death count in district i, educational group e, on day t; $f(T_{it}, \ell; \boldsymbol{\theta}_{ie})$ is a cross-basis function jointly modelling the non-linear exposure-response relationship and distributed lag effects of maximum daily temperature up to lag $\ell = 7$ days; $s(t; \boldsymbol{\varphi}_{ie})$ is a natural spline of time with 7 degrees of freedom per year, capturing long-term trends and seasonality; and $h_q(\cdot)$ are day-of-week indicators. The quasi-Poisson specification addresses overdispersion in mortality count data.

The temperature-response dimension was parametrised using quadratic B-splines with internal knots at the 10th, 75th, and 90th percentiles of each district's temperature distribution[4], yielding $p = 5$ basis functions. The lag dimension was modelled using natural splines with three internal knots at logarithmically-spaced intervals. The cross-basis was reduced to a cumulative exposure-response summary using `crossreduce` in R, yielding a vector of $p = 5$ reduced coefficients $\hat{\boldsymbol{\theta}}_{ie}$ and their associated variance-covariance matrix $\mathbf{S}_{ie}$.

B.2 Second-stage meta-regression

The reduced coefficients were passed to a multivariate mixed-effects meta-regression:

$$\hat{\boldsymbol{\theta}}_{ie} = X_{ie}\boldsymbol{\beta} + Z_i\mathbf{b}_i + \boldsymbol{\varepsilon}_{ie} \tag{B2}$$

where X_{ie} contains a linear term for educational attainment as the sole meta-predictor (selected by AIC; Figure B3a), $\boldsymbol{\beta}$ captures how educational attainment systematically shifts the exposure-response function, $Z_i\mathbf{b}_i$ are district-level random effects with $\mathbf{b}_i \sim \mathcal{N}(\mathbf{0}, \boldsymbol{\Psi})$, and $\boldsymbol{\varepsilon}_{ie} \sim \mathcal{N}(\mathbf{0}, \mathbf{S}_{ie})$ represents within-study error propagated from the first stage.

District-specific exposure-response functions were obtained via BLUPs (presented in Figure B2), which shrink district estimates toward the population average in proportion to first-stage uncertainty:

$$\hat{\xi}_{ie} = \hat{\boldsymbol{\Psi}}\, Z_i^\top \left(Z_i \hat{\boldsymbol{\Psi}} Z_i^\top + \mathbf{S}_{ie}\right)^{-1} \left(\hat{\boldsymbol{\theta}}_{ie} - X_{ie}\hat{\boldsymbol{\beta}}\right) \tag{B3}$$

$$\tilde{\boldsymbol{\theta}}_{ie} = X_{ie}\hat{\boldsymbol{\beta}} + \hat{\xi}_{ie} \tag{B4}$$

[4]Sensitivity to knot placement was assessed across three alternative specifications: (10th, 75th, 95th), (25th, 75th, 90th), and (10th, 50th, 90th) percentiles. The direction, magnitude, and significance of the educational gradient were consistent across all specifications.

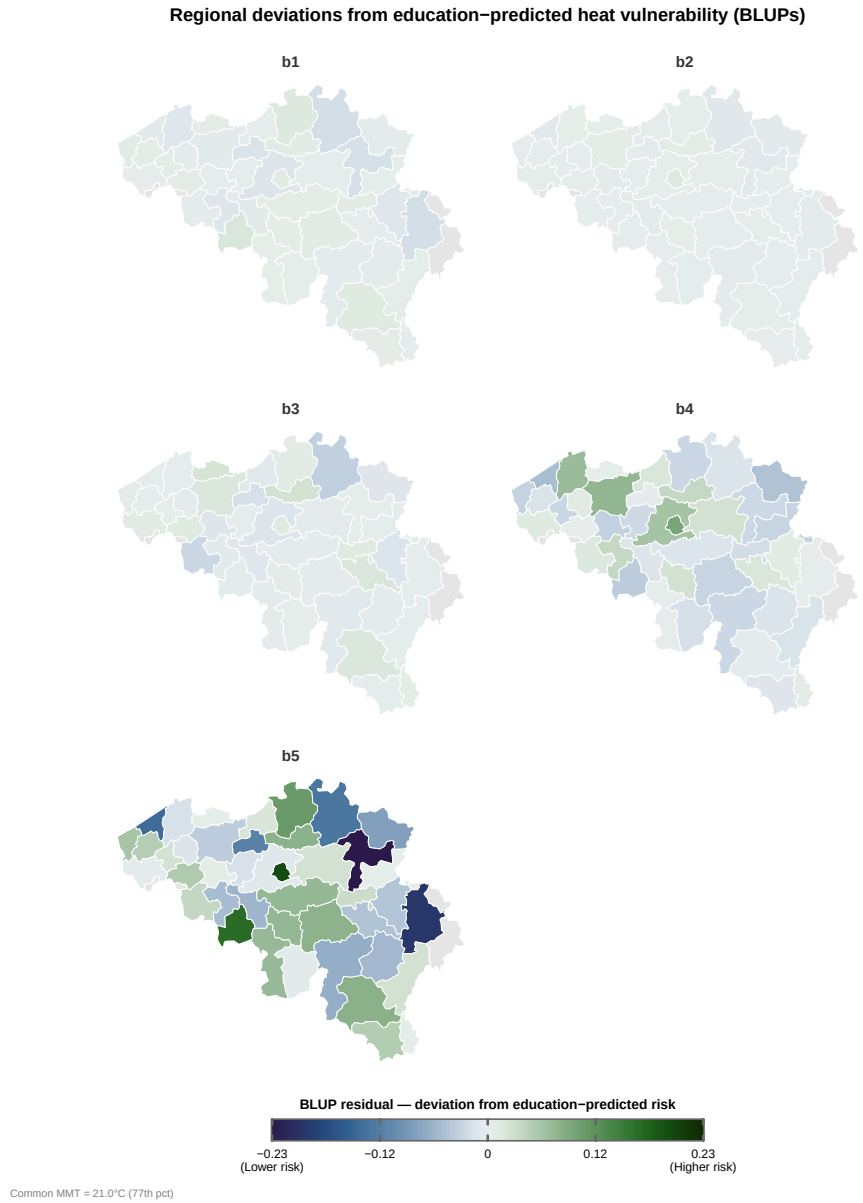

Fig. B2: Best Linear Unbiased Predictions by analytical district for each spline coefficient. Each map shows district-level random effects. Positive values indicate higher temperature risk than educational attainment alone predicts.

B.3 Age standardisation

For each district-education stratum, age-specific all-cause mortality rates were weighted by the national Belgian 2011 census age distribution to yield age-standardised all-cause rates. Heat-attributable rates were obtained as:

$$ASMR_{ia}^{heat} = AF_{ia} \times ASMR_{ia}^{allcause} \tag{B5}$$

B.4 Model selection

Model specification was determined through a grid search over two dimensions: the parametrisation of educational attainment (linear gradient vs. categorical) and the number of Partial Least Squares (PLS) components to retain as additional district-level meta-predictors. PLS regression was applied to the six domain-specific deprivation scores of the Belgian Index of Multiple Deprivation (Otavova et al. 2024) — covering income, employment, education, housing, crime, and health — to derive composite vulnerability indices that best explain variation in the temperature-mortality coefficients across districts. The correlation between BIMD domain scores and the retained PLS components is shown in Figure B3b, and illustrates the multidimensional structure of area-level deprivation captured by the index.

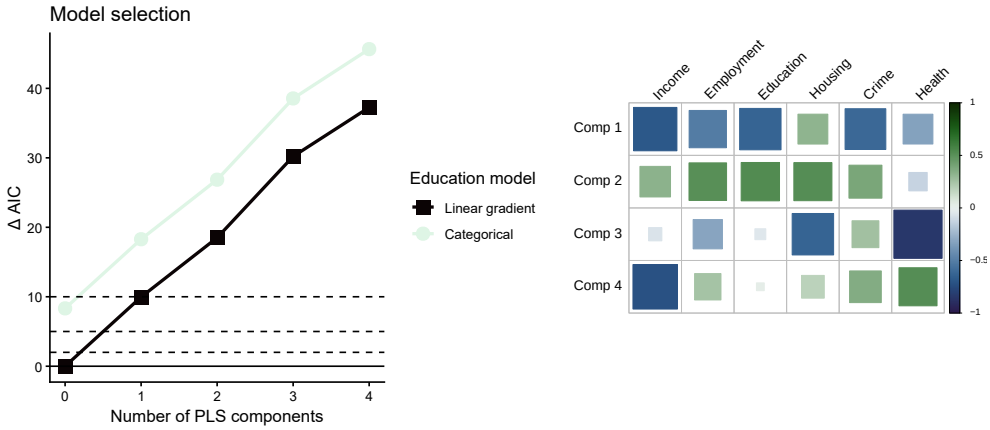

(a) Model selection for the second-stage meta-regression. ΔAIC relative to the best-fitting model is shown for each combination of education parameterisation and number of retained PLS deprivation components. Dashed horizontal lines indicate ΔAIC thresholds of 2, 5, and 10.

(b) Correlation between domain-specific deprivation scores from the Belgian Index of Multiple Deprivation and the retained PLS vulnerability components.

Fig. B3: Second-stage model specification.

The optimal specification was selected by Akaike Information Criterion (AIC) across all combinations of education parameterisation and number of retained PLS components (0 to 4), as shown in Figure B3a. A linear education gradient with no additional PLS components was selected as the best-fitting model (ΔAIC = 0). The incremental inclusion of PLS deprivation components did not improve model fit under either education parametrisation, indicating that the educational gradient alone adequately characterises between-district heterogeneity in heat vulnerability.

Appendix C Detailed results

Table C4: Relative risk of mortality at different temperature percentiles by educational attainment. All estimates relative to common MMT = 21.0°C (77th percentile).

		Relative Risk (95% CI)		
Percentile	Temp (°C)	Low	Secondary	Tertiary
1.0	-0.9	1.026 (1.002–1.052)	1.054 (1.023–1.086)	1.083 (1.024–1.145)
2.5	0.4	1.024 (1.002–1.047)	1.047 (1.019–1.076)	1.071 (1.019–1.126)
25.0	9.1	1.002 (0.984–1.022)	1.023 (1.000–1.046)	1.043 (1.000–1.088)
50.0	15.0	0.996 (0.983–1.010)	1.011 (0.994–1.028)	1.026 (0.995–1.058)
75.0	20.5	0.999 (0.998–1.000)	1.000 (0.999–1.002)	1.002 (0.999–1.004)
97.5	28.3	1.124 (1.099–1.149)	1.113 (1.084–1.143)	1.103 (1.052–1.156)
98.0	29.4	1.169 (1.142–1.197)	1.146 (1.115–1.178)	1.122 (1.070–1.178)
99.0	31.3	1.276 (1.242–1.311)	1.214 (1.176–1.253)	1.155 (1.094–1.221)

Note: RR = relative risk; 95% CI in parentheses. Rows above the horizontal rule correspond to temperatures below the MMT (cold range); rows below correspond to the heat range.

Table C5: Crude and age-standardised heat-attributable mortality rates during extreme heat (above 97.5th national temperature percentile, 28.3°C) by educational attainment, Belgian closed cohort 2002–2019.

Education	Crude rate (per 100,000 PY)	ASMR (95% CI)	Crude − ASMR
Low	24.98 (21.18–26.07)	26.46 (22.40–27.63)	-1.48
Secondary	12.57 (10.14–14.13)	19.37 (15.54–21.76)	-6.80
Tertiary	7.57 (4.65–9.96)	12.96 (7.97–17.04)	-5.39

Table C6: Age-standardised heat-attributable mortality rates (per 100,000 person-years) during extreme heat (above 97.5th national temperature percentile, 28.3°C) by district and educational attainment. Districts ordered by NUTS-3 code. Belgian closed cohort 2002–2019.

		ASMR (95% CI)		
Code	District	Low	Secondary	Tertiary
BE100	Brussels	33.48 (25.00–34.75)	26.16 (19.10–29.16)	19.85 (12.73–24.32)
BE211	Antwerp	25.30 (19.35–29.92)	19.06 (12.97–22.61)	11.88 (6.26–18.71)
BE212	Mechelen	29.48 (21.50–35.92)	22.28 (13.63–27.83)	14.82 (8.20–24.60)
BE213	Turnhout	27.91 (19.88–34.65)	19.41 (11.53–26.25)	10.83 (4.37–18.78)
BE221	Hasselt	23.57 (14.68–32.76)	18.52 (8.13–25.20)	10.81 (0.56–19.43)
BE222	Maaseik	26.98 (16.51–36.38)	17.43 (9.07–26.17)	13.11 (1.91–20.21)
BE223	Tongres	28.01 (19.39–36.80)	22.23 (11.76–29.78)	15.48 (3.73–21.35)
BE231	Aalst	23.13 (15.35–29.58)	16.76 (9.21–21.78)	11.39 (3.56–18.37)
BE232	Dendermonde	26.71 (16.88–34.21)	21.94 (10.67–26.16)	13.21 (3.91–22.42)
BE233	Eeklo	19.93 (12.56–24.67)	19.31 (8.01–20.89)	9.38 (2.36–16.80)
BE234	Ghent	25.52 (18.07–28.87)	19.76 (12.09–23.55)	13.50 (6.77–19.11)
BE235	Oudenaarde	25.95 (16.13–30.81)	16.55 (9.92–23.85)	12.00 (4.47–20.44)
BE236	Sint-Niklaas	27.86 (19.07–32.34)	18.48 (13.66–27.64)	14.95 (6.66–21.13)
BE241	Halle-Vilvoorde	28.73 (22.00–34.06)	21.08 (14.34–25.57)	14.17 (8.35–20.36)
BE242	Leuven	30.42 (23.00–36.49)	25.64 (15.60–29.50)	17.45 (8.59–23.42)
BE251	Bruges	20.27 (14.02–23.16)	16.25 (9.83–18.35)	12.00 (5.00–15.85)
BE252	Diksmuide	16.31 (11.98–24.18)	19.04 (9.24–21.96)	5.21 (2.94–15.84)
BE253	Ypres	18.05 (12.23–23.29)	11.41 (7.39–18.02)	12.33 (3.11–14.83)
BE254	Kortrijk	23.63 (16.12–29.23)	19.71 (10.28–23.09)	11.46 (4.60–17.54)
BE255	Ostend	10.99 (6.96–16.27)	10.07 (3.45–12.57)	5.88 (0.00–9.84)
BE256	Roeselare	21.97 (12.46–24.87)	13.24 (7.86–19.16)	10.97 (3.04–15.58)
BE257	Tielt	22.49 (16.02–29.31)	19.42 (10.11–23.21)	15.52 (5.30–22.35)
BE258	Veurne	13.59 (9.45–18.29)	8.29 (5.51–14.50)	8.46 (2.14–11.15)
BE310	Nivelles	29.64 (20.19–34.84)	23.09 (13.63–27.80)	13.85 (6.68–22.49)
BE321	Ath	27.76 (19.54–35.93)	22.36 (13.27–29.87)	17.18 (6.06–21.50)
BE322	Charleroi	30.71 (21.64–36.26)	24.37 (15.69–29.25)	15.29 (7.95–23.23)
BE323	Mons	32.01 (21.96–37.42)	22.83 (14.44–28.69)	18.19 (7.21–22.94)
BE325	Soignies	26.28 (17.19–34.07)	21.27 (10.34–26.74)	13.91 (4.90–22.61)
BE326	Thuin	30.31 (19.50–34.45)	21.88 (12.90–27.76)	15.12 (5.96–20.25)
BE324+BE327	Tournai-Mouscron	44.60 (31.04–52.39)	32.86 (19.35–37.66)	17.02 (9.10–27.54)
BE331	Huy	32.39 (19.53–39.12)	22.37 (11.81–29.65)	17.76 (4.79–22.55)
BE332	Liège	33.16 (24.40–37.90)	23.93 (16.25–30.49)	16.79 (7.86–24.72)
BE334	Waremme	33.17 (19.20–39.01)	23.99 (12.31–32.65)	16.22 (4.07–23.43)
BE335+BE336	Verviers	20.14 (12.28–23.95)	12.69 (6.19–18.35)	6.38 (0.00–12.81)
BE341	Arlon	28.60 (18.65–33.99)	21.15 (11.65–28.81)	8.99 (3.96–21.38)
BE342	Bastogne	24.50 (15.05–28.31)	9.64 (8.95–22.15)	8.00 (1.61–15.46)
BE343	Marche-en-Famenne	25.56 (17.01–32.69)	11.76 (9.30–24.58)	8.17 (1.83–17.10)
BE344	Neufchâteau	24.53 (16.06–28.56)	16.94 (9.29–21.67)	10.81 (3.15–16.68)
BE345	Virton	35.63 (21.69–40.18)	17.71 (13.91–33.12)	16.77 (5.30–23.27)
BE351	Dinant	27.15 (17.76–33.87)	20.50 (10.73–27.82)	11.26 (2.79–21.80)
BE352	Namur	27.07 (19.44–33.40)	22.61 (13.45–27.14)	16.23 (5.80–20.52)
BE353	Philippeville	27.94 (16.11–33.94)	19.60 (10.96–28.62)	11.77 (2.75–17.96)

Appendix D Sensitivity analyses

D.1 Handling missing educational attainment data

A total of 16.8% of deaths in the study period had no recorded educational attainment. To assess the sensitivity of our results to this missing data, we tested two alternative assignment strategies. The first assigns all deaths with unknown educational attainment to the low education group, representing a scenario under the assumption that unknown attainment is disproportionately concentrated among individuals with little formal education. The second distributes unknown deaths proportionally across the three educational groups according to the observed distribution of deaths within each district.

Results are presented in Figure D4. The exposure-response functions remain broadly stable across all three specifications. Under proportional assignment, the secondary and tertiary curves shift upward slightly relative to the main analysis, as a share of unknown deaths is redistributed to these groups. Under the low-assignment scenario, the low education curve rises modestly while the secondary and tertiary curves are unchanged. The educational gradient in the extreme heat tail remains consistent across all specifications, and the significance of the education effect on the extreme heat spline coefficient is preserved.

Unknown deaths were excluded from the main analysis given the impossibility of verifying their true educational attainment, but their inclusion under either assumption does not alter the conclusions.

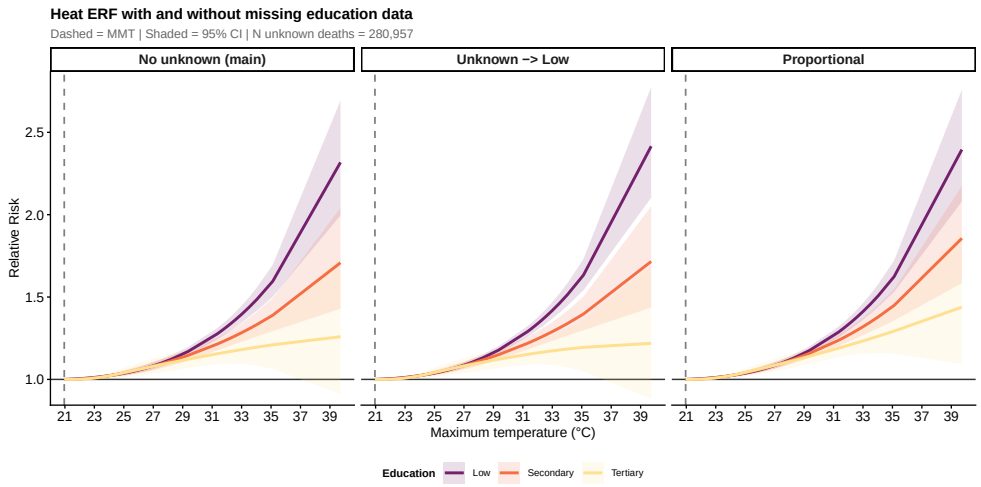

Fig. D4: Heat exposure-response functions by educational attainment under three specifications: main analysis (no NAs), assignment of all unknown deaths to the low education group, and proportional assignment based on the observed district-level distribution of deaths.

D.2 Lag definition and lagged effects of heat on mortality

The choice of lag length in DLNMs depends on the biological mechanism that are being studied. Heat-related mortality is known to occur rapidly following exposure as discussed in Section 1.1. For this reason, the main analysis uses a maximum lag of seven days. To verify that this choice does not affect our conclusions, we repeated the analysis using lags of 14 and 21 days and compared the resulting exposure-response functions in the heat range.

Figure D5 shows that longer lag specifications produce wider confidence intervals in the heat range, as the model attributes deaths over an extended window where few additional heat-related deaths are biologically expected. The MMT rises with lag length — from 21°C at lag 7 to 24.5°C at lag 21 — likely because longer lags capture cold-related displacement effects that compress the cold part of the curve, though the practical impact is limited given the near-null relative risks in this temperature range. Across all three specifications, the direction and ordering of the educational gradient are preserved, with the low education group consistently showing higher relative risks at extreme temperatures than the secondary and tertiary groups.

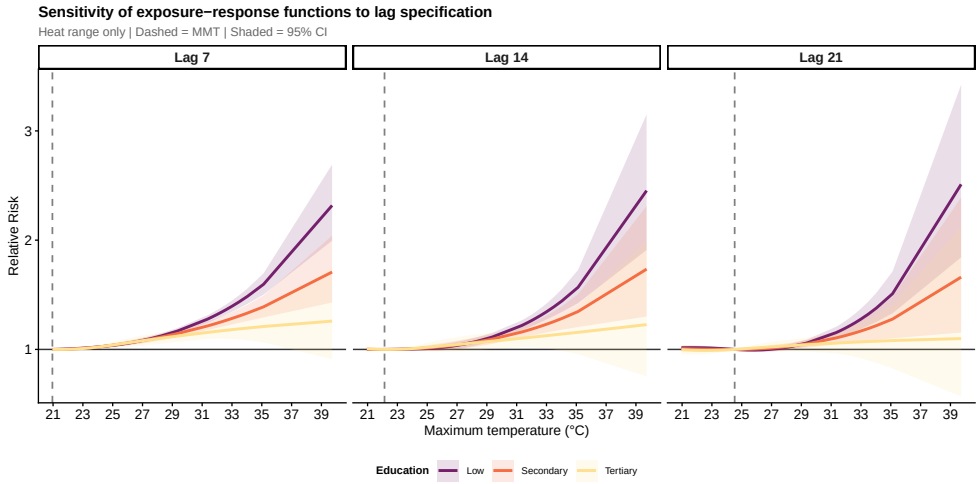

Fig. D5: Heat exposure-response functions by educational attainment and lag specification (7, 14, and 21 days). Results are shown for the heat range only, above the common MMT. Shaded areas represent 95% confidence intervals. Longer lag specifications produce wider uncertainty bounds without altering the direction or ordering of the educational gradient.

The structure of the lagged effect is further illustrated in Figure D6, which shows the lag-specific relative risk at different temperature percentiles for a lag of seven days. Across all percentiles, the highest relative risks occur within the first two days following a hot day, with the excess risk dissipating rapidly and becoming negligible beyond

day five or six. This pattern is consistent with the short biological timescale of heat-related mortality and confirms that a seven-day lag captures the relevant exposure window without introducing noise from longer periods where no physiological effect is expected.

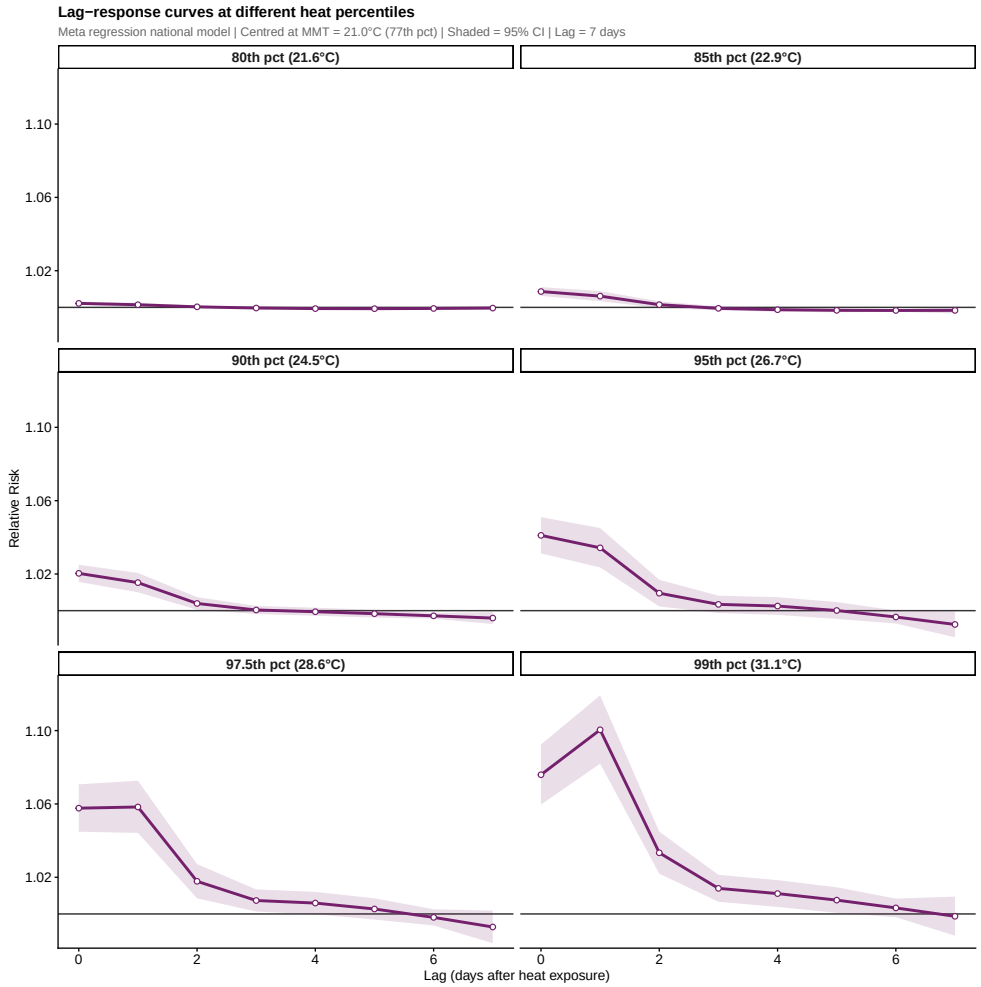

Fig. D6: Lag-specific relative risk of mortality at different national temperature percentiles (80th to 99th), estimated from a national pooled model with a maximum lag of seven days. Each panel shows how the relative risk evolves over the days following a day at the indicated temperature, relative to the minimum mortality temperature (MMT = 21°C). Shaded areas represent 95% confidence intervals.

References

Anderson, B.G., Bell, M.L.: Weather-Related Mortality: How Heat, Cold, and Heat Waves Affect Mortality in the United States **20**(2), 205–213 (2009) 20485691. Accessed 2026-04-27

Alahmad, B., Khraishah, H., Royé, D., Vicedo-Cabrera, A.M., Guo, Y., Papatheodorou, S.I., Achilleos, S., Acquaotta, F., Armstrong, B., Bell, M.L., Pan, S.-C., Sousa Zanotti Stagliorio Coelho, M., Colistro, V., Dang, T.N., Van Dung, D., De' Donato, F.K., Entezari, A., Guo, Y.-L.L., Hashizume, M., Honda, Y., Indermitte, E., Íñiguez, C., Jaakkola, J.J.K., Kim, H., Lavigne, E., Lee, W., Li, S., Madureira, J., Mayvaneh, F., Orru, H., Overcenco, A., Ragettli, M.S., Ryti, N.R.I., Saldiva, P.H.N., Scovronick, N., Seposo, X., Sera, F., Silva, S.P., Stafoggia, M., Tobias, A., Garshick, E., Bernstein, A.S., Zanobetti, A., Schwartz, J., Gasparrini, A., Koutrakis, P.: Associations between extreme temperatures and cardiovascular cause-specific mortality: Results from 27 countries **147**(1), 35–46 (2023) https://doi.org/10.1161/CIRCULATIONAHA.122.061832 . Publisher: American Heart Association. Accessed 2025-07-18

Benmarhnia, T., Deguen, S., Kaufman, J.S., Smargiassi, A.: Review article: Vulnerability to heat-related mortality: A systematic review, meta-analysis, and meta-regression analysis **26**(6), 781 (2015) https://doi.org/10.1097/EDE.0000000000000375 . Accessed 2025-08-23

Balaj, M., Henson, C.A., Aronsson, A., Aravkin, A., Beck, K., Degail, C., Donadello, L., Eikemo, K., Friedman, J., Giouleka, A., Gradeci, I., Hay, S.I., Jensen, M.R., Mclaughlin, S.A., Mullany, E.C., O'connell, E.M., Sripada, K., Stonkute, D., Sorensen, R.J.D., Solhaug, S., Vonen, H.D., Westby, C., Zheng, P., Mohammad, T., Eikemo, T.A., Gakidou, E.: Effects of education on adult mortality: a global systematic review and meta-analysis **9**(3), 155–165 (2024) https://doi.org/10.1016/S2468-2667(23)00306-7 . Publisher: Elsevier. Accessed 2025-07-18

Barnett, A.G., Tong, S., Clements, A.C.A.: What measure of temperature is the best predictor of mortality? **110**(6), 604–611 (2010) https://doi.org/10.1016/j.envres.2010.05.006 . Accessed 2025-07-18

Calvin, K., Dasgupta, D., Krinner, G., Mukherji, A., Thorne, P.W., Trisos, C., Romero, J., Aldunce, P., Barret, K., Blanco, G., Cheung, W.W.L., Connors, S.L., Denton, F., Diongue-Niang, A., Dodman, D., Garschagen, M., Geden, O., Hayward, B., Jones, C., Jotzo, F., Krug, T., Lasco, R., Lee, Y.-Y., Masson-Delmotte, V., Meinshausen, M., Mintenbeck, K., Mokssit, A., Otto, F.E.L., Pathak, M., Pirani, A., Poloczanska, E., Pörtner, H.-O., Revi, A., Roberts, D.C., Roy, J., Ruane, A.C., Skea, J., Shukla, P.R., Slade, R., Slangen, A., Sokona, Y., Sörensson, A.A., Tignor, M., Van Vuuren, D., Wei, Y.-M., Winkler, H., Zhai, P., Zommers, Z., Hourcade, J.-C., Johnson, F.X., Pachauri, S., Simpson, N.P., Singh, C., Thomas, A., Totin, E., Alegría, A., Armour, K., Bednar-Friedl, B., Blok, K., Cissé, G., Dentener,

F., Eriksen, S., Fischer, E., Garner, G., Guivarch, C., Haasnoot, M., Hansen, G., Hauser, M., Hawkins, E., Hermans, T., Kopp, R., Leprince-Ringuet, N., Lewis, J., Ley, D., Ludden, C., Niamir, L., Nicholls, Z., Some, S., Szopa, S., Trewin, B., Van Der Wijst, K.-I., Winter, G., Witting, M., Birt, A., Ha, M., Arias, P., Bustamante, M., Elgizouli, I., Flato, G., Howden, M., Méndez-Vallejo, C., Pereira, J.J., Pichs-Madruga, R., Rose, S.K., Saheb, Y., Sánchez Rodríguez, R., Ürge-Vorsatz, D., Xiao, C., Yassaa, N., Romero, J., Kim, J., Haites, E.F., Jung, Y., Stavins, R., Birt, A., Ha, M., Orendain, D.J.A., Ignon, L., Park, S., Park, Y.: IPCC, 2023: Climate Change 2023: Synthesis Report, Summary for Policymakers. Contribution of Working Groups I, II and III to the Sixth Assessment Report of the Intergovernmental Panel on Climate Change [Core Writing Team, H. Lee and J. Romero (eds.)]. IPCC, Geneva, Switzerland. https://doi.org/10.59327/ipcc/ar6-9789291691647.001 . https://www.ipcc.ch/report/ar6/syr/ Accessed 2025-07-20

Conte Keivabu, R.: Extreme temperature and mortality by educational attainment in spain, 2012–2018 **38**(5), 1145–1182 (2022) https://doi.org/10.1007/s10680-022-09641-4 . Accessed 2024-11-08

Conte Keivabu, R., Basellini, U., Zagheni, E.: Racial disparities in deaths related to extreme temperatures in the united states **7**(9), 1630–1637 (2024) https://doi.org/10.1016/j.oneear.2024.08.013 . Accessed 2024-11-08

Crouzier, C., Van Schaeybroeck, B., Duchêne, F., Duchêne, M., Hamdi, R., Kirakoya-Samadoulougou, F., Demoury, C.: The impact of climate and demographic changes on future mortality in brussels, belgium **236**, 261–267 (2024) https://doi.org/10.1016/j.puhe.2024.07.028 . Accessed 2024-11-08

Demoury, C., Aerts, R., Vandeninden, B., Van Schaeybroeck, B., De Clercq, E.M.: Impact of Short-Term Exposure to Extreme Temperatures on Mortality: A Multi-City Study in Belgium **19**(7), 3763 (2022) https://doi.org/10.3390/ijerph19073763 35409447. Accessed 2026-03-27

Demoury, C., De Troeyer, K., Berete, F., Aerts, R., Van Schaeybroeck, B., Heyden, J., De Clercq, E.M.: Association between temperature and natural mortality in belgium: Effect modification by individual characteristics and residential environment **851**, 158336 (2022) https://doi.org/10.1016/j.scitotenv.2022.158336 . Accessed 2024-12-16

De Grande, H., Vandenheede, H., Deboosere, P.: Trends in young-adult mortality between the 1990s and the 2000s in urban and non-urban areas in belgium: The role of a changing educational composition in overall mortality decline **30**, 61–69 (2014) https://doi.org/10.1016/j.healthplace.2014.08.003 . Accessed 2025-07-18

Schrijver, E., Bundo, M., Ragettli, M.S., Sera, F., Gasparrini, A., Franco, O.H., Vicedo-Cabrera, A.M.: Nationwide analysis of the heat- and cold-related mortality trends in switzerland between 1969 and 2017: The role of population aging **130**(3), 037001 (2022) https://doi.org/10.1289/EHP9835 . Publisher: Environmental Health

Perspectives. Accessed 2025-07-18

Ellena, M., Ballester, J., Mercogliano, P., Ferracin, E., Barbato, G., Costa, G., Ingole, V.: Social inequalities in heat-attributable mortality in the city of Turin, northwest of Italy: A time series analysis from 1982 to 2018. Environmental Health **19**(1), 116 (2020) https://doi.org/10.1186/s12940-020-00667-x

Eggerickx, T., Sanderson, J.-P., Vandeschrick, C.: Mortality in belgium from nineteenth century to today: Variations according to age, sex, and social and spatial contexts **8**(2), 7–59 (2020) https://doi.org/10.14428/rqj2020.08.02.01 . Number: 2. Accessed 2025-07-18

Fan, Z.-y., Yang, Y., Zhang, F.: Association between health literacy and mortality: a systematic review and meta-analysis **79**(1), 119 (2021) https://doi.org/10.1186/s13690-021-00648-7 . Accessed 2025-07-18

Gosling, S.N., Lowe, J.A., McGregor, G.R., Pelling, M., Malamud, B.D.: Associations between elevated atmospheric temperature and human mortality: a critical review of the literature **92**(3), 299–341 (2009) https://doi.org/10.1007/s10584-008-9441-x . Accessed 2024-10-30

Gagnon, D., Schlader, Z.J., Jay, O.: The Physiology behind the Epidemiology of Heat-Related Health Impacts **41**(1), 30–42 (2026) https://doi.org/10.1152/physiol.00012.2025 . Accessed 2026-04-27

Huang, J., Brink, H., Groot, W.: A meta-analysis of the effect of education on social capital **28**(4), 454–464 (2009) https://doi.org/10.1016/j.econedurev.2008.03.004 . Accessed 2025-07-19

Janoš, T., Quijal-Zamorano, M., Shartova, N., Gallo, E., Méndez Turrubiates, R.F., Denisse Beltrán Barrón, N., Peyrusse, F., Ballester, J.: Heat-related mortality in Europe during 2024 and health emergency forecasting to reduce preventable deaths **31**(12), 4065–4074 (2025) https://doi.org/10.1038/s41591-025-03954-7 . Accessed 2026-04-28

Lüthi, S., Fairless, C., Fischer, E.M., Scovronick, N., Ben Armstrong, Coelho, M.D.S.Z.S., Guo, Y.L., Guo, Y., Honda, Y., Huber, V., Kyselý, J., Lavigne, E., Royé, D., Ryti, N., Silva, S., Urban, A., Gasparrini, A., Bresch, D.N., Vicedo-Cabrera, A.M.: Rapid increase in the risk of heat-related mortality **14**(1), 4894 (2023) https://doi.org/10.1038/s41467-023-40599-x . Accessed 2026-04-27

Lutz, W., Muttarak, R.: Forecasting societies' adaptive capacities through a demographic metabolism model **7**(3), 177–184 (2017) https://doi.org/10.1038/nclimate3222 . Publisher: Springer Science and Business Media LLC. Accessed 2025-07-19

Lee, M.K., Rega, E., Loopmans, M., Otavova, M., Van Orshoven, J., Aerts, R.,

Somers, B.: Socioeconomic inequities in visible, functional, and accessible green space exposure: A cross-sectional study in Flanders, Belgium **118**, 129301 (2026) https://doi.org/10.1016/j.ufug.2026.129301 . Accessed 2026-04-29

Marí-Dell'Olmo, M., Tobías, A., Gómez-Gutiérrez, A., Rodríguez-Sanz, M., Olalla, P., Camprubí, E., Gasparrini, A., Borrell, C.: Social inequalities in the association between temperature and mortality in a south european context **64**(1), 27–37 (2019) https://doi.org/10.1007/s00038-018-1094-6 . Accessed 2024-10-30

Masselot, P., Gasparrini, A.: Modelling extensions for multi-location studies in environmental epidemiology **34**(3), 615–629 (2025) https://doi.org/10.1177/09622802241313284 . Accessed 2025-07-21

Otavova, M., Masquelier, B., Faes, C., Borre, L., Bouland, C., De Clercq, E., Vandeninden, B., De Bleser, A., Devleesschauwer, B.: Measuring small-area level deprivation in belgium: The belgian index of multiple deprivation **45**, 100587 (2023) https://doi.org/10.1016/j.sste.2023.100587

Otavova, M., Masquelier, B., Faes, C., Borre, L., Vandeninden, B., Clercq, E., Devleesschauwer, B.: Trends in socioeconomic inequalities in cause-specific premature mortality in belgium, 1998–2019 **24**(1), 470 (2024) https://doi.org/10.1186/s12889-024-17933-z . Accessed 2025-01-09

Renard, F., Devleesschauwer, B., Gadeyne, S., Tafforeau, J., Deboosere, P.: Educational inequalities in premature mortality by region in the Belgian population in the 2000s **75**(1), 44 (2017) https://doi.org/10.1186/s13690-017-0212-x . Accessed 2026-04-29

Son, J.-Y., Liu, J.C., Bell, M.L.: Temperature-related mortality: a systematic review and investigation of effect modifiers **14**(7), 073004 (2019) https://doi.org/10.1088/1748-9326/ab1cdb . Publisher: IOP Publishing. Accessed 2025-07-20

Van Hemelrijck, W.M.J., Willaert, D., Gadeyne, S.: The geographic pattern of belgian mortality: can socio-economic characteristics explain area differences? **74**(1), 22 (2016) https://doi.org/10.1186/s13690-016-0135-y . Accessed 2025-07-18

Willem, L., Kerckhove, K.V., Chao, D.L., Hens, N., Beutels, P.: A Nice Day for an Infection? Weather Conditions and Social Contact Patterns Relevant to Influenza Transmission **7**(11), 48695 (2012) https://doi.org/10.1371/journal.pone.0048695 . Accessed 2026-04-27

Xu, Z., FitzGerald, G., Guo, Y., Jalaludin, B., Tong, S.: Impact of heatwave on mortality under different heatwave definitions: A systematic review and meta-analysis **89-90**, 193–203 (2016) https://doi.org/10.1016/j.envint.2016.02.007 . Accessed 2024-10-30

Yin, Q., Wang, J., Ren, Z., Li, J., Guo, Y.: Mapping the increased minimum mortality

temperatures in the context of global climate change **10**(1), 4640 (2019) https://doi.org/10.1038/s41467-019-12663-y . Publisher: Nature Publishing Group. Accessed 2025-07-18

Zhao, Q., Guo, Y., Ye, T., Gasparrini, A., Tong, S., Overcenco, A., Urban, A., Schneider, A., Entezari, A., Vicedo-Cabrera, A.M., Zanobetti, A., Analitis, A., Zeka, A., Tobias, A., Nunes, B., Alahmad, B., Armstrong, B., Forsberg, B., Pan, S.-C., Íñiguez, C., Ameling, C., Valencia, C.D.l.C., Åström, C., Houthuijs, D., Dung, D.V., Royé, D., Indermitte, E., Lavigne, E., Mayvaneh, F., Acquaotta, F., de'Donato, F., Ruscio, F.D., Sera, F., Carrasco-Escobar, G., Kan, H., Orru, H., Kim, H., Holobaca, I.-H., Kyselý, J., Madureira, J., Schwartz, J., Jaakkola, J.J.K., Katsouyanni, K., Diaz, M.H., Ragettli, M.S., Hashizume, M., Pascal, M., Coélho, M.d.S.Z.S., Ortega, N.V., Ryti, N., Scovronick, N., Michelozzi, P., Correa, P.M., Goodman, P., Saldiva, P.H.N., Abrutzky, R., Osorio, S., Rao, S., Fratianni, S., Dang, T.N., Colistro, V., Huber, V., Lee, W., Seposo, X., Honda, Y., Guo, Y.L., Bell, M.L., Li, S.: Global, regional, and national burden of mortality associated with non-optimal ambient temperatures from 2000 to 2019: a three-stage modelling study **5**(7), 415–425 (2021) https://doi.org/10.1016/S2542-5196(21)00081-4 . Publisher: Elsevier. Accessed 2025-07-18